Dinuclear Gold(III) Complexes as Potential Anticancer Agents: Structure, Reactivity and Biological Profile of a Series of Gold(III) Oxo-Bridged Derivatives

Chiara Gabbiani[1], Annalisa Guerri[1], Maria Agostina Cinellu[2] and Luigi Messori[1,*]

[1]*Dipartimento di Chimica and CRIST, Centro Interdipartimentale di Cristallografia Strutturale, Università di Firenze, Polo Scientifico, Via della Lastruccia 3, 50019 Sesto Fiorentino, Firenze, Italy*

[2]*Dipartimento di Chimica, Università di Sassari, Via Vienna 2, 07100 Sassari, Italy*

Abstract: Six homologous gold(III) dinuclear oxo-bridged complexes, of the type $[(bipy^{nR})Au(\mu\text{-}O)_2Au(bipy^{nR})][PF_6]_2$, bearing variously substituted 2,2'-bipyridine ligands ($bipy^{nR}$ = 2,2'-bipyridine, 4,4'-di-tert-butyl-, 6-methyl-, 6-neopentyl-, 6-*o*-*xylyl*- and 6,6'-dimethyl-2,2'-bipyridine), here called *Auoxos*, were prepared, characterised and recently tested as potential anticancer agents. Crystal structures were obtained for five members of the series that allowed us to perform detailed comparative analyses. Interestingly, the various *Auoxos* showed an acceptable stability profile in buffer solution and turned out to manifest outstanding antitumor properties *in vitro*. In particular, one member of this family, Auoxo6 ($bipy^{nR}$ = 6,6'-dimethyl-2,2'-bipyridine), produced more selective and far greater antiproliferative effects than all other tested *Auoxos*, qualifying itself as the best "drug candidate". In turn, COMPARE analysis of the cytotoxicity profiles of five *Auoxos*, toward an established panel of thirty-six human tumor cell lines, revealed important mechanistic differences; a number of likely biomolecular targets could thus be proposed such as HDAC and PKC. Biophysical studies revealed markedly different modes of interaction with calf thymus DNA for two representative Auoxo compounds. In addition, a peculiar reactivity with model proteins was documented on the ground of spectrophotometric and ESI MS data, most likely as the result of redox processes. In view of the several experimental evidences gathered so far, it can be stated that *Auoxos* constitute a novel family of promising cytotoxic gold compounds with an innovative mechanism of action that merit a more extensive pharmacological evaluation.

Keywords: Anticancer drugs, X-ray structures, gold complexes, cytotoxic activity, mechanisms of action, gold protein complexes, gold DNA complexes.

1. INTRODUCTION

Gold compounds are increasingly attracting researchers' attention as a source of novel cytotoxic substances, of potential use in cancer treatment. In particular, several gold(III) compounds, with profoundly different molecular structures, have been designed, synthesized and tested as antiproliferative agents during the last decade [1-5]. Very relevant cytotoxic properties were disclosed for many gold(III) compounds and initial structure-function relationships outlined [6-8]. From those studies, it emerged rather clearly that gold(III) compounds must be considered, in general, as *prodrugs* and that their biological activities, subsequent to chemical activation, primarily arise from gold coordination to specific sites of target biomolecules or, alternatively, from gold-centred redox reactions and consequent oxidative damage. However, some notable exceptions to this rule were reported as well (see, for instance, the case of stable gold(III) porphyrins) [8]. It is also evident that the relevant cytotoxic effects produced by gold(III) compounds are afforded, in most cases, through biochemical mechanisms that are substantially different from those typical of platinum drugs and essentially "DNA independent" [1]. The occurrence of a different mechanism of action seems to be a very attractive feature for this novel class of *cytotoxics* as it might lead to the development of novel drugs capable of overcoming the severe problem of cisplatin (CDDP) resistance.

As the molecular framework of the metal apparently plays a crucial role in modulating the overall chemical and biological reactivity of the metal centre itself, appropriate and increasingly sophisticated chemical architectures need to be designed and built up for the improvement of the pharmacological properties of these metallodrugs [9, 10]. In recent years, a rather common strategy in the field of "*Anticancer metal based drugs*" has been the design of dinuclear or polynuclear derivatives [11]. Such a "multinuclear" strategy produced promising results in the case of anticancer platinum drugs [12] and was recently extended to non-platinum compounds such as ruthenium compounds [13]. We have applied this synthetic approach to gold(III) compounds and prepared a series of dinuclear complexes, named *Auoxos*, characterised by the presence of a Au_2O_2 "diamond" core and of variously substituted 2,2'-bipyridyl

*Address correspondence to this author at the Dipartimento di Chimica and CRIST, Centro Interdipartimentale di Cristallografia Strutturale, Università di Firenze, Polo Scientifico, *Via* della Lastruccia 3, 50019 Sesto Fiorentino, Firenze, Italy; Tel: +39 055 4573388; Fax: +39 055 4573385;
E-mail: luigi.messori@unifi.it

1874-8465/10 2010 Bentham Open

ligands (bipy^{nR}) [14]. We describe here the main features of the synthesis, the structural chemistry, the reactivity and the biological properties of this novel family of gold-based agents, as they emerge from our recent investigations. The perspectives for their future use as anticancer agents will be also discussed.

2. DESIGN AND SYNTHESIS OF *AUOXO* COMPOUNDS

A few years ago we evaluated the biological properties of the mononuclear square planar gold(III) compound [Au(bipy)(OH)$_2$][PF$_6$], AuOH1, featuring a chelating 2,2'-bipyridine and two hydroxo groups as ligands. AuOH1 was found to manifest appreciable cytotoxic properties against a few standard human tumor cell lines; however, we noticed that its stability in aqueous solutions was rather poor and not very adequate for pharmaceutical purposes. A substantial improvement in terms of stability in solution (mainly with respect to ligand substitution reactions) could be obtained as the result of the condensation reaction of two AuOH1 units to give the dinuclear oxo-bridged derivative [(bipy)Au(μ-O)$_2$Au(bipy)][PF$_6$]$_2$, *Auoxo1*. Interestingly, this reaction may be reverted by refluxing *Auoxo1* in water over several hours. In Fig. (**1**) AuOH1 and its dinuclear derivative *Auoxo1* are schematically represented.

Unfortunately, "duplication" of the starting compound, while producing a higher stability in solution, did not result into significantly improved performances in terms of cytotoxicity.

Nonetheless, upon introduction of various substituents on the 2,2'-bipyridine backbone, we were able to modulate the pharmacological properties of the dinuclear parent compound. As a result of this strategy, five further oxo bridged complexes of the type [(bipy^{nR})Au(μ-O)$_2$Au(bipy^{nR})][PF$_6$]$_2$ (bipy^{nR} = 4,4'-di-tert-butyl-2,2'-bipyridine, *Auoxo2*; 6-methyl-2,2'-bipyridine, *Auoxo3*; 6neopentyl-2,2'-bipyridine, *Auoxo4*; 6-o-xylyl-2,2'-bipyridine, *Auoxo5*; 6,6'-dimethyl-2,2'bipyridine, *Auoxo6*) (Fig. **2**) were prepared and fully characterized; afterward, some aspects of their biological properties were investigated in depth [14].

Auoxo2 was prepared according to the same procedure used for *Auoxo1*, i.e. by the condensation reaction of the dihydroxo complex [Au(bipy^{2tBu})(OH)$_2$][PF$_6$], AuOH2. At variance, *Auoxo3-Auoxo6* were obtained by reaction of the neutral adducts [Au(bipy^{nR})Cl$_3$] with NaOAc and excess K[PF$_6$] in aqueous solution. *Auoxo3* was obtained as a ca. 1:1 mixture of the cis and trans isomers, while, in the case of *Auoxo4* and *Auoxo5*, only trans isomers were formed. In this short review accounts of those studies are given.

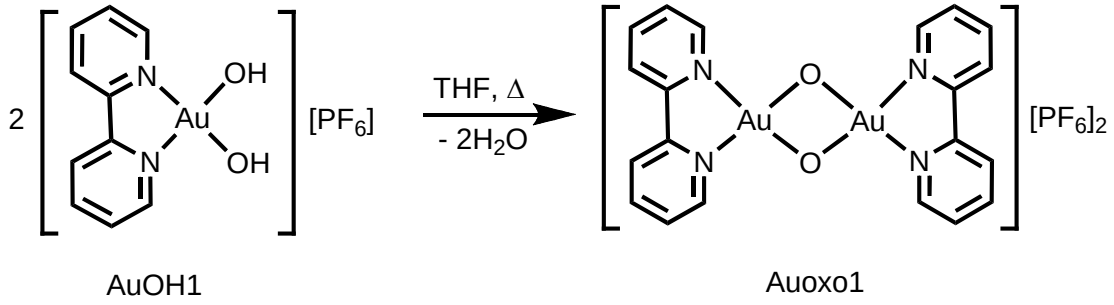

Fig. (1). Schematic drawing of the synthesis of *Auoxo1*.

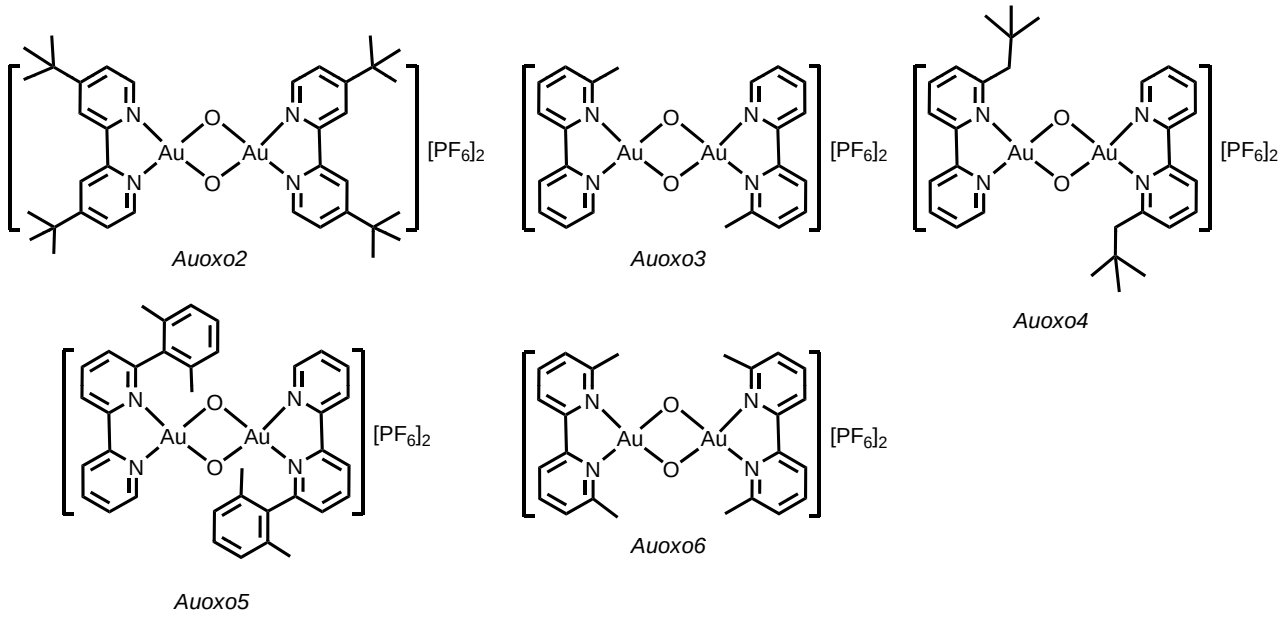

Fig. (2). *Auoxos*. Note: *Auoxo3* is a ca.1:1 mixture of the cis and trans isomers (the latter is represented in the figure).

3. STRUCTURAL CHARACTERISATION

The solid state X-ray crystal structures of five compounds of the series (namely *Auoxo1*, cis-*Auoxo3*, *Auoxo4*, *Auoxo5*, and *Auoxo6*) are now available [15]. Despite numerous attempts, crystals of *Auoxo2*, $[(bipy^{2tBu})Au(\mu\text{-}O)_2Au(bipy^{2tBu})][PF_6]_2$, could not be obtained. The crystal structures for four *Auoxo* compounds, recently solved in our laboratory, are depicted in Fig. (**3**).

The metal complex, two hexafluorophosphate (PF_6^-) anions, and one acetonitrile molecule are present in the asymmetric unit of cis-*Auoxo3*. In those of *Auoxo1* and *Auoxo5* half of the metallic cation, one PF_6^- anion and one acetonitrile solvent molecule are found. In the asymmetric unit of *Auoxo6*, one fourth of the metal complex and half of a hexafluorophosphate anion have been identified. Upon considering the structure of *Auoxo4***,** reported in a previous study [16], all these binuclear gold(III) compounds have in common the approximately planar "diamond core" system Au_2O_2 and the bipyridyl rings of the ligands. With this in mind, and taking the *Auoxo1* complex as the reference compound for the whole series, structural parameters of *Auoxo1*, cis-*Auoxo3*, *Auoxo4*, *Auoxo5*, and *Auoxo6* were analysed (reported in Table **1**) in such a way to highlight the effects on them of the different substituents.

The "diamond core" system", that is planar because of the inversion centre in *Auoxo1*, *Auoxo5*, and *Auoxo6* [15] and because the deviation is not significant for *Auoxo3*, shows an interesting trend relating the Au···Au and O···O distances across the series of examined compounds. As reported in Table **1**, while the distance between the two gold atoms increases along the series (in the order *Auoxo1* < *Auoxo5* < cis-*Auoxo3* < *Auoxo4* < *Auoxo6*), the corresponding O···O distance decreases. This grouping is coplanar with the five-membered ring formed by Au(1)−N(1)−C(5)−C(6)[C(5′)]−N(2)[N(1′)] in each complex [and by the Au(2)−N(3)−C(16) −C(17)−N(4) ring in cis-*Auoxo3*]; the maximum deviation is 2.5(2)° in the case of cis-*Auoxo3*. In *Auoxo6* the two planes form an angle of 6.44(9)°. Moreover, in *Auoxo5*, the xylyl ring and the bipyridine moiety are almost perpendicular (76.1(2)°). When considering each metal centre, the coordination is basically planar, the largest deviation from the best plane containing the coordination ion being found for Au(1) in *Auoxo5* (0.14 Å out of the plane).

The distances between the two metal atoms vary from 2.96 to 3.04 Å. These values are shorter than the sum of the van der Waals radii for two gold atoms (3.60 Å), even shorter than those found for other dinuclear complexes, e.g. $Au_2(XR_n)_2$ (XRn = NR2, OR, SR, Cl, Br), [15, 17] implying the occurrence of a weak Au···Au interaction. Indeed, theoretical studies revealed that the strength of gold-gold interactions largely depends on the gold oxidation state and that appreciable metal-metal interactions occur when both gold centres are in the oxidation state +3 [18].

Upon analysing the influence of the alkyl or aryl substituents of the bipirydiyl rings, at position 6, on the coordination bond lengths, it may be pointed out that, in cis-*Auoxo3*, trans-*Auoxo5*, and *Auoxo6*, they cause a significant increase in the Au−N distance adjacent to the substituent itself (e.g., to 2.07 Å in *Auoxo6*) in comparison to *Auoxo1***.** The other Au−N distance in both cis-*Auoxo3* and *Auoxo5* remains nearly unchanged; the same trend was found in *Auoxo4*. At variance with the Au-N distances, the Au−O bond lengths do not vary appreciably (1.97 Å), and this latter value is in agreement with the same distance found for mononuclear gold(III) alkoxo complexes supported by 2,2′-bipyridines [15]. The only exception is the O(1)−Au(2) bond length in complex *Auoxo3* which is significantly shorter.

The occurrence of substituents on the bipyridyl rings, in position 6, also affects the N−Au−O angle facing the substituent itself. In the reference compound *Auoxo1*, the angles N(1)−Au(1)−O(1) and N(2)−Au(1)−O(2) are 98.1(2)° and 98.8(2)°, respectively. In *Auoxo6* they both measure 102.3(3)°; in cis-*Auoxo3* and *Auoxo5* the N(2)−Au(1)−O(2)[O(1′)] angles [and N(4)−Au(2)−O(2) in cis-*Auoxo3*] are larger than N(1)−Au(1)−O(1) and cis- *Auoxo3* N(3)−Au(2)−O(1)]: ca 105 vs ca 95°. The increased Au−N bond dis-

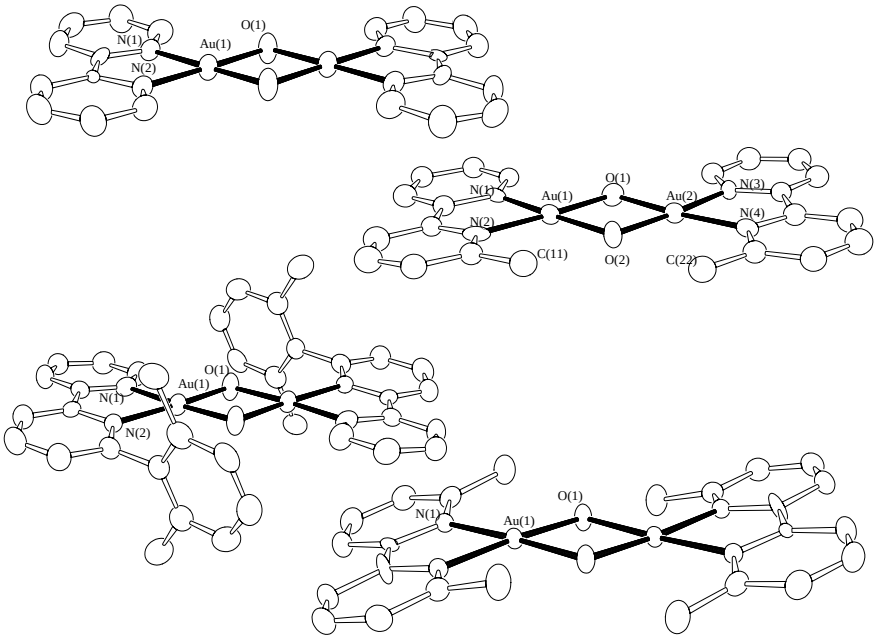

Fig. (3). The crystal structures of *Auoxo1* (**a**), *Auoxo3* (**b**), *Auoxo5* (**c**) and *Auoxo6* (**d**).

Table 1. Selected Bond Distances (Å) and Angles (°) for Compounds *Auoxo-1*, *-2*, *-3* and *-4*

	Auoxo1	*Auoxo3*	*Auoxo5*	*Auoxo6*
Au(1)-Au(2)[Au(1')][a]	2.9573(6)	3.0165(7)	2.9963(6)	3.044(1)
Au(1)-O(1)	1.971(5)	1.972(7)	1.962(6)	1.955(5)
Au(1)-O(2)[O(1')][a]	1.957(6)	1.976(7)	1.977(6)	
Au(1)-N(1)	2.015(4)	1.99(1)	2.023(7)	2.065(6)
Au(1)-N(2)	2.000(4)	2.071(9)	2.081(7)	
Au(2)-O(1)		1.931(7)		
Au(2)-O(2)		1.975(7)		
Au(2)-N(3)		2.017(9)		
Au(2)-N(4)		2.028(9)		
Au(1)-O(1)-Au(2)[Au(1')][a]	97.7(2)	101.2(3)	99.0(2)	102.3(3)
O(1)-Au(1)-N(1)	98.1(2)	95.4(3)	94.7(3)	100.8(3)
O(1)-Au(1)-N(2)	178.9(2)	175.8(3)	174.3(2)	
O(1)-Au(1)-O(2)[O(1')][a]	82.3(2)	79.1(3)	81.0(2)	77.7(3)
N(1)-Au(1)-N(2)[N(1")][a]	80.8(2)	80.4(4)	79.6(3)	80.4(4)
N(1)-Au(1)-O2[O(1')][a]	179.2(2)	174.2(3)	175.6(2)	176.3(2)
N(2)-Au(1)-O(2)[O(1')][a]	98.8(2)	105.1(3)	104.8(2)	
O(1)-Au(2)-N(3)		95.2(3)		
O(1)-Au(2)-N(4)		174.5(3)		
O(1)-Au(2)-O(2)		80.1(3)		
N(3)-Au(2)-N(4)		79.6(4)		
N(3)-Au(2)-O(2)		175.3(3)		
N(4)-Au(2)-O(2)		105.0(3)		

[a] Symmetry operations are as follows. *Auoxo-1*: ' = -x,-y+1,-z; *-3*: ' = -x,-y,-z+1; *-4*: ' = -x,-y,-z; " = x,-y,z.

tance and the larger N−Au−O angle most likely arise from the steric hindrance of the substituent. In nice agreement with this interpretation, short intermolecular contacts are detected in cis-*Auoxo3* and *Auoxo6*, connecting the methyl pendant arms *via* a weak hydrogen bond: in cis- *Auoxo3*, O(2) is 2.88 Å far apart from C(11) and 2.84 Å from C(22), while in *Auoxo6*, the C(6)···O(1) contact is 2.81 Å.

Due to the presence of many aromatic systems, in the lattice of cis-*Auoxo3* and *Auoxo5*, different intramolecular and intermolecular interactions were identified. "Offset π-stacked" interactions in cis-*Auoxo3* involve the geometric centroids of the aromatic rings Ct2 and Ct3 (this latter belongs to a molecule related by −x + 1, −y, −z): the distance for the stacked aromatic rings is 4.03 Å. In *Auoxo5* this kind of interaction involves the xylyl rings of the original molecule and the molecule related by −x, −y, −z, the distance being 4.06 Å. Also CH/π interactions can be identified in the crystal lattice of the two above mentioned compounds. In cis-*Auoxo3* the hydrogen atom H(11a) points directly to the centre (Ct1) of the aromatic ring of a molecule related by −x + 1, −y, −z, the distance between them is 2.84 Å. In *Auoxo5* this kind of interaction is intramolecular and involves H(1) of the bipyridine ligand and the xylyl ring of the same molecule: the distance H(1)···Ct1 is 2.99 Å. Moreover, in cis-*Auoxo3*, an intermolecular interaction of 3.45 Å is found between Au(2) and O(2′) of a symmetry-related molecule (reported by −x + 1, −y, −z).

4. THE SOLUTION BEHAVIOUR

The solution chemistry of the various *Auoxo* compounds was initially investigated through absorption UV−visible spectroscopy, upon consideration of their favourable optical properties. Notably, all six compounds are soluble and stable in DMSO, with retention of their characteristic binuclear structure. Accordingly, concentrated DMSO solutions of each binuclear gold(III) compound (1×10^{-2} M) were prepared and then diluted into a standard 10 mM phosphate buffer, pH 7.4, to a final concentration of $5\text{-}10\times10^{-5}$ M. The resulting samples were monitored spectrophotometrically over 24 h at 37 °C providing the spectral profiles that are shown in Fig. (**4**). Notably, all six compounds (dissolved in DMSO) exhibit intense absorptions in the 300−400 nm re-

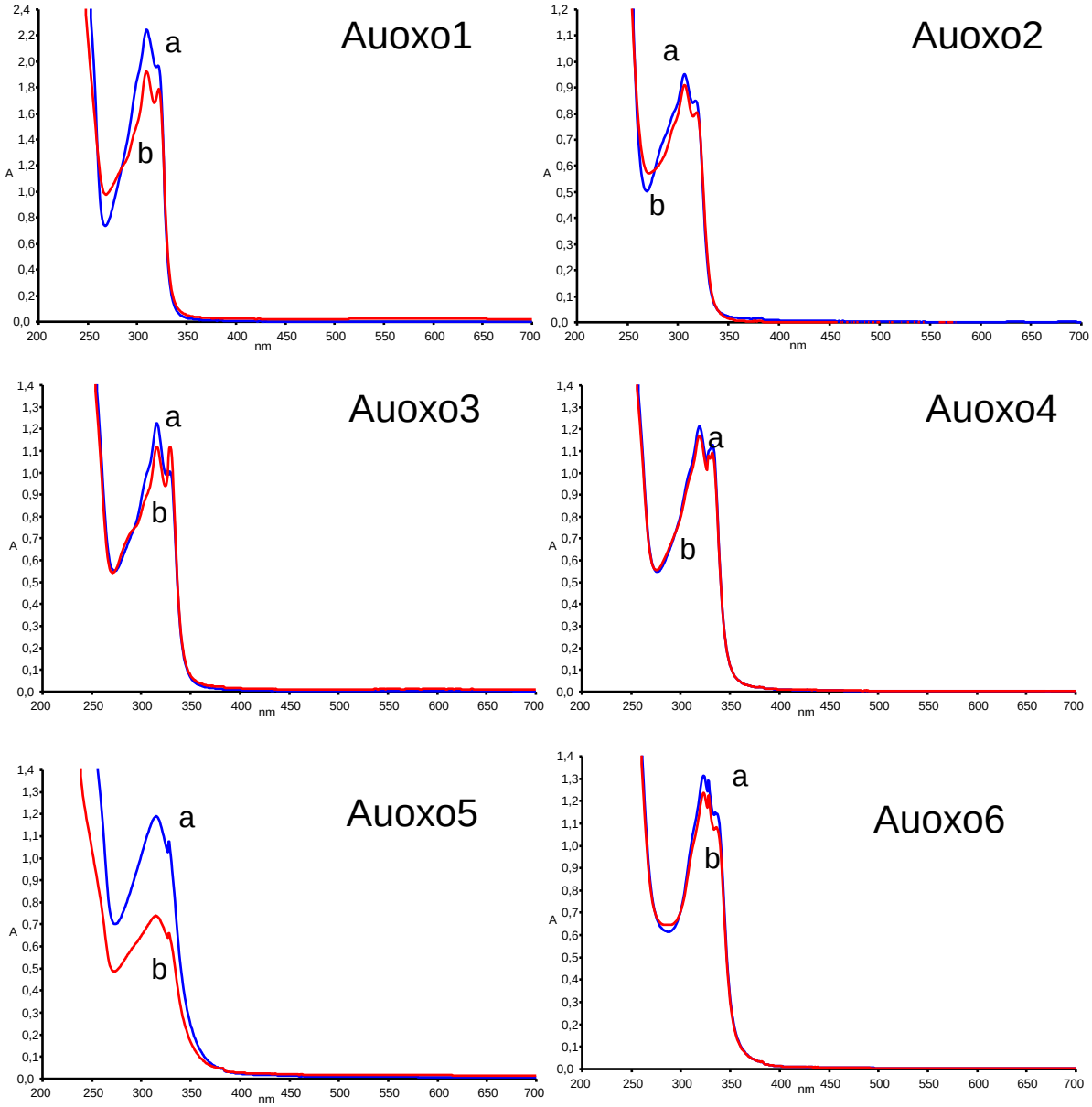

Fig. (4). Hydrolysis profiles of *Auoxos*, in 10 mM phosphate, pH 7.4, at 37 °C; t = 0 (**a**) and t = 24 h (**b**).

gion, straightforwardly assigned as LMCT bands. Upon dilution within the standard phosphate buffer, these transitions keep roughly unmodified in shape over 24 h observation (r), implying a substantial stability of the various dinuclear gold(III) chromophores. Nonetheless, some small spectral changes were noticed with time, probably related to the occurrence of initial hydrolysis processes and/or to the formation of some oligomeric species. In any case, the dinuclear species remain dominant in buffered aqueous solutions, for several hours. At variance with the other complexes, *Auoxo5* manifested a progressive decrease in the intensity of its major LMCT band, at 310 nm. After 24 h, this band dropped to 60% of its initial intensity, without any significant shape modification. However, these relevant spectral changes could later be ascribed to the occurrence of precipitation phenomena and were reversed by modifying the composition of the medium (i.e. by increasing the amount of DMSO).

Extensive cleavage of the oxo bridges could only be achieved by applying far more drastic solution conditions. For instance, nearly complete conversion of *Auoxo1* into its monomeric $[Au(bipy)(OH)_2]^+$ species (AuOH1) could be afforded after 2 h of incubation at 70°C [15].

The stability of the various *Auoxo* compounds toward representative biological reductants was also assayed [14]. Ascorbic acid (AscA) was chosen as a typical reducing agent due to its widespread occurrence within biological fluids. Notably, addition of AscA, in a twofold molar excess, caused fast reduction of all six dinuclear gold(III) compounds. The occurrence of gold(III) reduction was clearly witnessed by disappearance of the LMCT bands, characteristic of the gold(III) bipyridyl chromophore; concomitantly, a broad absorption band showed up around 550 nm that is attributed to the formation of colloidal gold, one of the typical products of gold(III) reduction. For comparison purposes, the effects of glutathione (GSH) on the various *Auoxos* were

also evaluated [14]. Similarly to ascorbic acid, GSH caused rapid disappearance of the characteristic LMCT bands, in agreement with gold(III) reduction. However, in contrast to the case of ascorbic acid, colloidal gold did not form. Most likely, the presence of an excess of glutathione favours the formation of soluble gold(I) thiolate species as a major product of gold(III) reduction in the place of colloidal gold [19]. The overall results, obtained so far, disclose an appreciable sensitivity of *Auoxos* toward even mildly reducing conditions, suggesting that these compounds, within the cellular milieu, undergo, very likely, reduction to gold(I) or to colloidal gold.

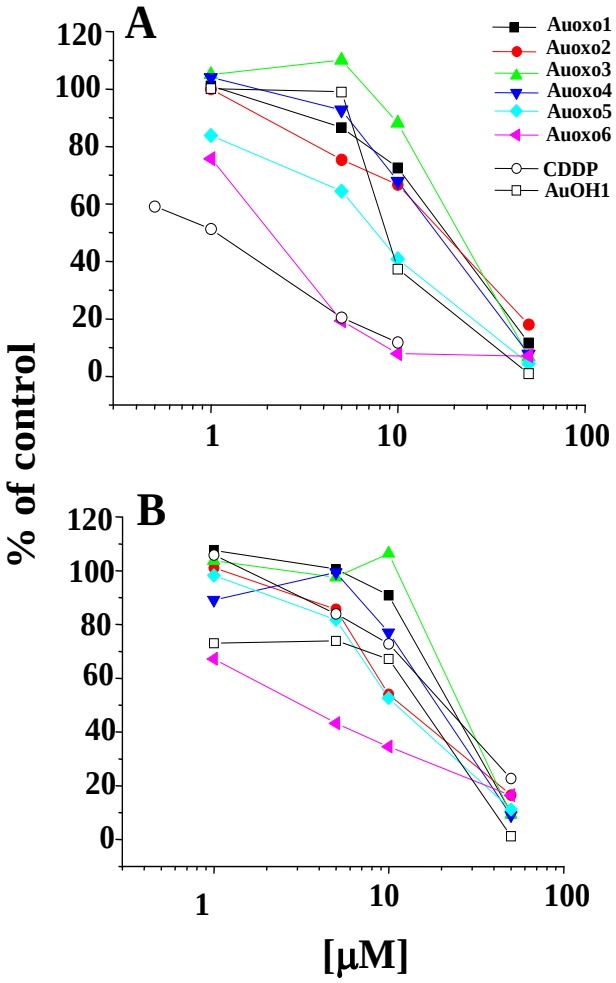

Fig. (5). Antiproliferative effects of *Auoxo*s toward A2780/S (**A**) or A2780/R (**B**).

5. THE ANTIPROLIFERATIVE PROPERTIES

The acceptable stability of the *Auoxos,* in aqueous solution, under physiological-like conditions, allowed us to perform an extensive testing of their antiproliferative properties *in vitro*. Initially, the cytotoxic properties of the *Auoxo* compounds were assayed against the A2780 ovarian carcinoma human cell line, either sensitive (A2780/S) or resistant (A2780/R) to CDDP, according to the standard procedure described by Skehan *et al*. [20].

Relevant cytotoxicity profiles and IC50 data are shown in Fig. (**5**) and Table **2** respectively. For comparison purposes the antiproliferative effects of the mononuclear precursor AuOH1 and of CDDP on the same cell lines are also reported.

Notably, most *Auoxos* (*Auoxo1*−*Auoxo5*) were found to display remarkable and roughly comparable antiproliferative effects, with IC_{50} values typically falling in the 10−30 μM range; no relevant cross resistance with CDDP was highlighted. In contrast, *Auoxo6* turned out to be far more active than all other complexes on both cell lines, with IC_{50} values of ca 2 μM for the sensitive line and ca 5 μM for the resistant one. It follows that *Auoxo6* is about 5 times more active than CDDP on the CDDP resistant line.

Afterward, the *Auoxo* compounds were analyzed at Oncotest (Freiburg, Germany) according to specific screening strategies of new anticancer agents, as previously described (see http://www.oncotest.de) [21]. Initially, a standard 12-cell-line panel was used, which allowed the various compounds to be ranked according to their average cytotoxic potency. Then, the best performers were challenged on a wider 36-cell-line panel. This latter experiment, carried out on four *Auoxo* compounds (the best performers in the biological tests, i.e. *Auoxo1*, *Auoxo4*, *Auoxo5* and *Auoxo6*), allowed us to assess, with a high reliability, the selectivity of the observed antitumor effects. The representative pattern of antiproliferative properties measured for *Auoxo6* is shown in Fig. (**6**). Important differences were evident in their respective cytotoxic potencies and tumor selectivities as summarised in Table **3**. Again, *Auoxo6* turned out to be the most active compound and to display appreciable tumor selectivity. These properties make *Auoxo6* -by far- the most promising member of the series.

Finally, the results of the 36-cell-line experiments were analysed through the COMPARE algorithm [22, 23], to gain specific mechanistic information on each complex. Activity patterns of the assayed compounds were correlated to the patterns of the approximately 100 reference compounds with a known mechanism of action, tested in the Oncotest 36-cell-line panel. Similarity in the cytotoxicity pattern is often

Table 2. IC_{50} Values of *Auoxos* Toward A2780 Cells in Comparison to AuOH1 and Cisplatin (CDDP)

	IC_{50} (μM)							
Cell Lines	**CDDP**	**AuOH1**	***Auoxo1***	***Auoxo2***	***Auoxo3***	***Auoxo4***	***Auoxo5***	***Auoxo6***
A2780/S	2.1±0.2	8.4±0.1	22.8±1.5	12.1±1.5	25.4±2.5	12.7±1.1	11.0±1.5	1.79±0.17
A2780/R	24.4±0.1	14.9±0.3	23.3±0.4	13.5±1.8	29.8±3.1	19.8±1.8	13.2±1.2	4.8± 0.5

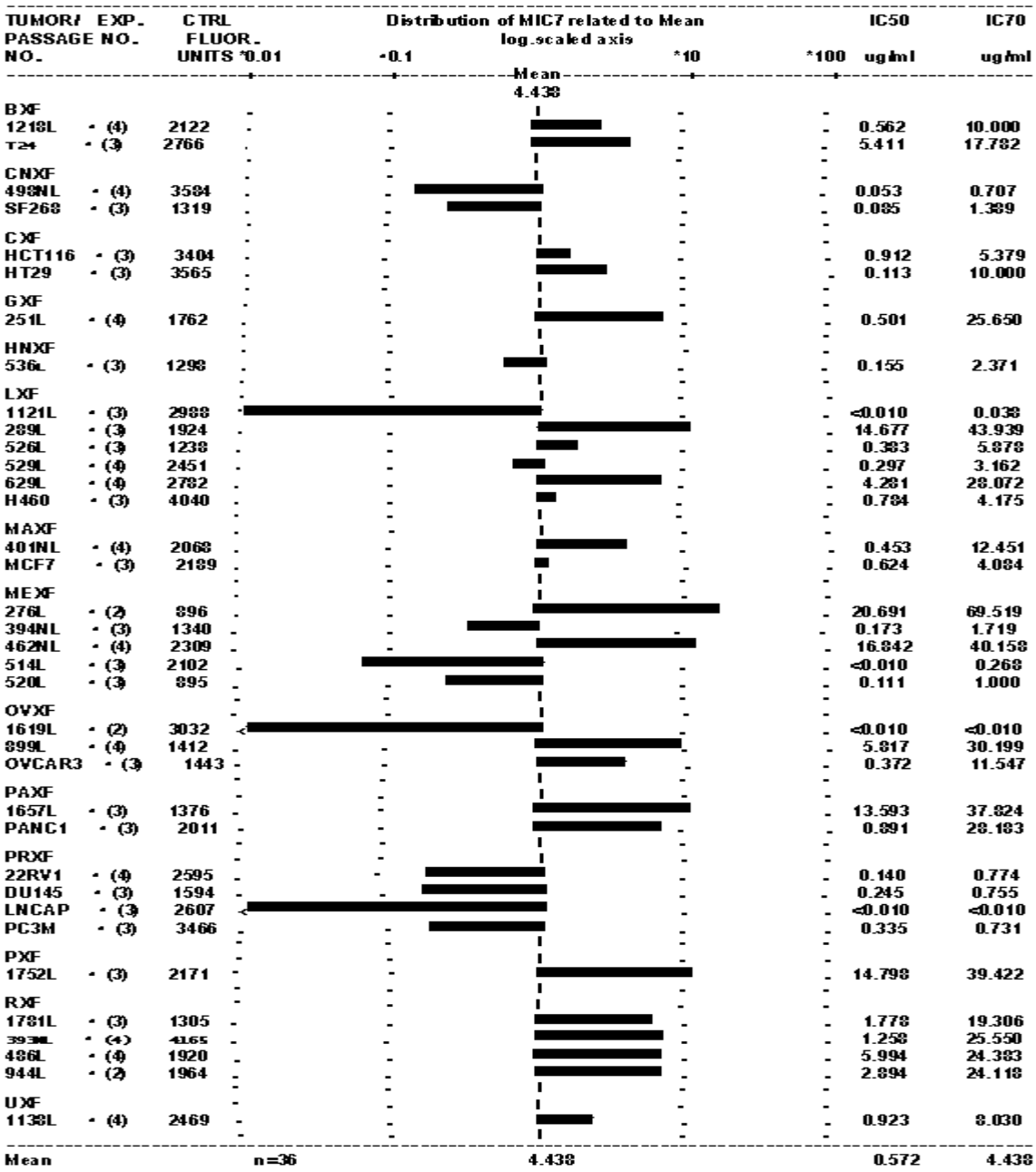

Fig. (6). Anticancer profile of *Auoxo6* in a panel of 36 cell lines (IC_{70} mean graph) [21]. IC_{50} represents the amount of drug necessary to inhibit the cell growth by 50%. IC_{70} is the drug concentration that induces a 70% cell growth inhibition.

associated to similarity in the mechanism of action, in the resistance profile, and possibly in molecular structure [24].

Overall, this kind of approach is aimed at establishing initial structure-function relationships, of potential interest for further drug design and development. COMPARE analysis applied to the above *Auoxo* compounds provided quite interesting results (Table **3**). In general, these results were less homogeneous than it could be expected on the basis of the strict structural similarity existing among the various *Auoxos*.

Auoxo6 revealed striking similarities to various histone deacetylase (HDAC) inhibitors, i.e. ρ=0.72 for both the benzamide acetyldinaline and the cyclic peptide apicidin and ρ=0.61 for suberic bishydroxamate on the IC_{70} level [25]. *Auoxo1* showed a nearly identical IC_{70} profile to AuOH1. A Spearman rank correlation [26] of the IC_{70} profiles of the latter two compounds revealed ρ=0.91, indicating a strong similarity in their respective biological behaviour. This finding might be reasonably explained by assuming that *Auoxo1*, in the cellular milieu, may break down and convert into its monomeric form AuOH1. Pair wise, their potencies on the level of the mean IC_{50} and IC_{70} values were similar. COMPARE analysis indicated inhibition of protein kinase C (PKC) as the likely mechanism for their biological action. In fact, for both compounds, the PKC inhibitor UCN-01 (7-hydroxystaurosporine) reached the top scoring (ρ=0.68 for AuOH1 and ρ=0.65 for *Auoxo1* on the IC_{70} level). *Auoxo4* (mean IC_{70}=22 μg/ml) exhibited a relatively weak potency, and a remarkable tumor selectivity profile; no positive corre-

Table 3. ***In vitro*** **Anticancer Potency, Tumor Selectivity, and COMPARE Analysis for Selected *Auoxos***

Compound	Potency		Tumor Selectivity			Indicated *MoA* by COMPARE Analysis
	Mean IC_{50} (μg/ml)	Mean IC_{70} (μg/ml)	Selective/Total	Selective (%)	Rating	
Auoxo1	10.7	24.3	5/36	14	++	*PKC* inhibition
Auoxo4	8.76	21.8	4/36	11	++	Negative
Auoxo5	4.45	13.1	2/36	6	+	*HDAC* inhibition
Auoxo6	0.572	4.44	10/36	28	+++	*HDAC* inhibition

MoA mechanism of action, *HDAC* histone deacetylase, *PKC* protein kinase C.

lation to any of the 110 reference compounds was detected by COMPARE analysis (ρ<0.6). *Auoxo5* (mean IC_{70}=13 μg/ml), though less potent, was suggested to behave as an HDAC inhibitor.

Very remarkably, a poor correlation was typically found between the antiproliferative effects of the various *Auoxos* and the cytotoxicity profile of CDDP implying that their respective modes of action are very different. These findings appear to be in good agreement with recent studies suggesting that gold compounds produce their biological effects through a mitochondrial mechanism while not causing any direct DNA damage.

Thus, on the ground of the ONCOTEST protocol and of the predictions of COMPARE analysis, two probable biomolecular targets have been identified for *Auoxo* compounds, HDACs and PKc. HDACs form indeed an interesting new family of protein targets for anticancer compounds that were never proposed before as candidate targets for gold compounds [26]. At variance, it is worth remembering that Regala *et al*. recently suggested that a specific protein kinase c might be a target for the gold(I) compound aurothiomalate and might be of interest for cancer treatment [27].

6. MECHANISTIC STUDIES: REACTIONS WITH NUCLEIC ACIDS AND MODEL PROTEINS

To gain further insight into the specific reactivity of these novel gold(III) compounds with potential biomolecular targets, the reaction patterns of two representative members of the family i.e. Auoxo1 and Auoxo6, with calf thymus DNA and with a few model proteins were analyzed in detail by a variety of biophysical methods.

6.1. Reactions with Calf Thymus DNA

The interactions of *Auoxo1* and *Auoxo6* with calf thymus DNA were assayed according to an established protocol that couples spectroscopic and analytical determinations [14]. More in detail, *Auoxo1* and *Auoxo6* were dissolved in the reference phosphate buffer, at 37°C, and an appropriate amount of calf thymus DNA was added to both samples in such a way to reach r = 0.1 final stoichiometry (where r is the gold compound/base pair ratio). Afterward, samples were analyzed continuously over 24 h. Highly different spectroscopic patterns were observed in the two cases. Indeed, very modest perturbations of the characteristic spectral features of *Auoxo1* were seen after addition of calf thymus DNA (see Fig. **7A**): the bands characteristic of the gold(III) chromophore were substantially stable over 24 h observation. After this period, extensive ultrafiltration of the sample led to nearly complete separation of the gold(III) species (which crosses the membrane and moves to the lower fraction) from calf thymus DNA (which remains in the upper fraction) (Fig. **7A**, inset). Notably, the UV−visible spectrum of the gold(III) species, that is recovered in the lower fraction, matches rather closely the spectrum of *Auoxo1* in the phosphate buffer.

In contrast, in the case of *Auoxo6*, upon performing the same kind of experiments, a progressive decrease in intensity and significant modifications of the bands assigned to the gold(III) chromophore were observed over 24 h (Fig. **7B**). At the end of this period, extensive ultrafiltration failed to separate the gold-containing species from DNA. Substantial gold binding to DNA was instead demonstrated and then independently confirmed by inductively coupled plasma optical emission spectroscopy (ICP-OES) measurements (more than 80% of total gold was found associated with DNA).

Such a different behaviour toward calf thymus DNA was later confirmed by UV circular dichroism measurements. Circular dichroism is indeed a very suitable method to monitor the conformational state of the DNA double helix in solution and the effects produced by gold drugs [28]. Calf thymus DNA, in its native B-type conformation, is characterized by a positive band at 275 nm and a negative one at ca 242 nm. Remarkably, addition of *Auoxo1* to a solution of calf thymus DNA, at r = 0.1, produced only modest alterations of the CD spectrum. Some decrease in the intensity of the negative band at 242 nm was noticed that could be ascribed to a partial loss of DNA helicity (possibly due to occurrence of electrostatic interactions between the exposed phosphate groups and the positively charged metal complex). However, the above CD changes could be reversed nearly completely by ultrafiltration against the buffer, implying that the *Auoxo1*/calf thymus DNA interaction is weak and reversible in nature. At variance, *Auoxo6* resulted to be far more effective than *Auoxo1* in altering the CD spectra of B-type DNA. For instance, at r = 0.1, a more pronounced decrease of the negative CD band was detected coupled to a significant change of the positive band at 275 nm. This latter modification could be ascribed to an alteration in the overall base stacking of the double helix. Most remarkably, in the case of *Auoxo6*, a weak "induced" CD band also appeared at 345 nm. All these spectral modifications are diagnostic of

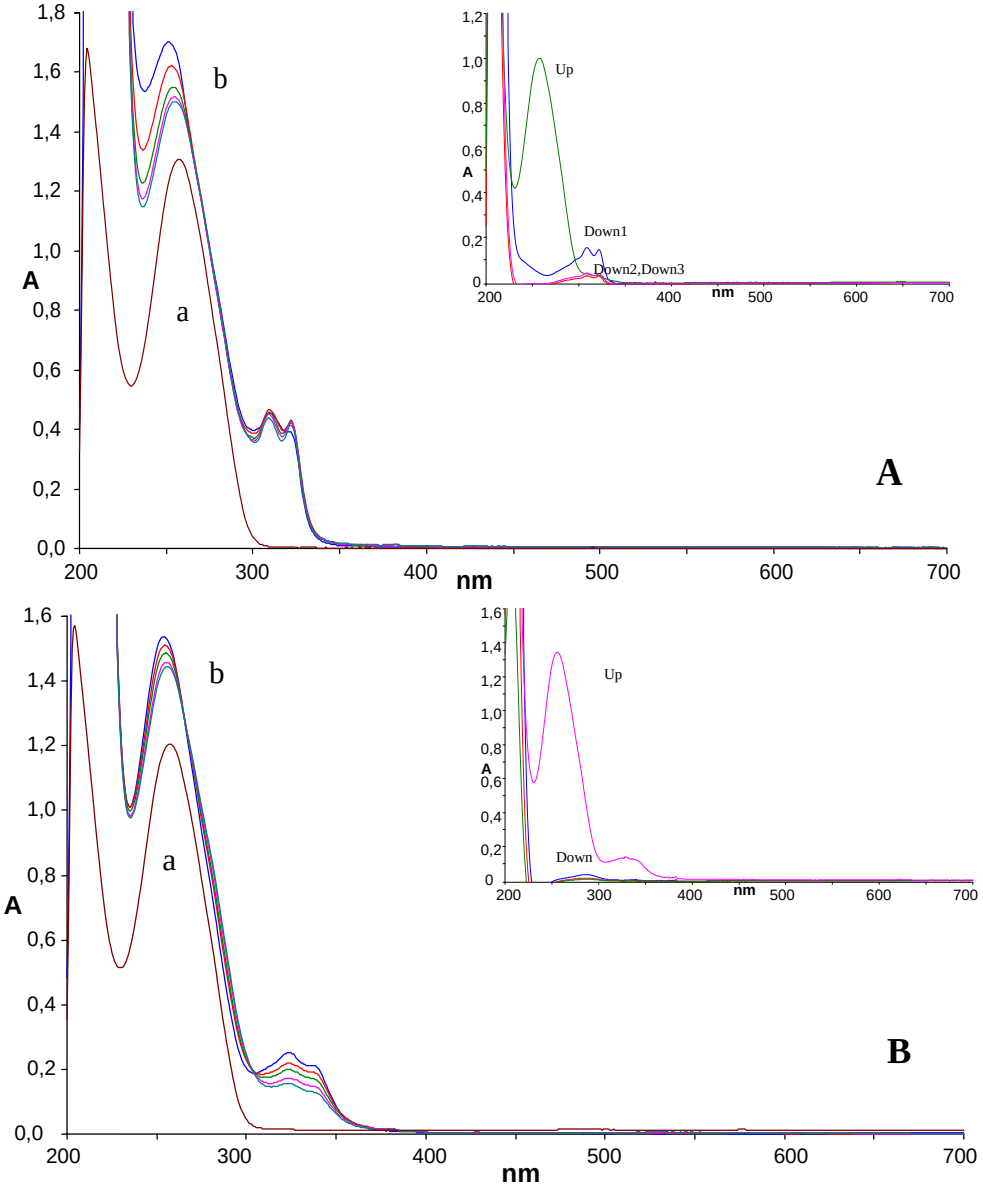

Fig. (7). Time-dependent spectral profiles for *Auoxo*/DNA adducts at the r = 0.1 stoichiometric ratio. The electronic spectra of 10^{-5} M calf thymus DNA were recorded before (a) and after (b) addition of *Auoxo1* (**A**) and *Auoxo6* (**B**) and were followed for 24 h at 37 °C. Results of ultrafiltration are shown in the insets.

the formation of a relatively stable *Auoxo6*/DNA adduct. No significant further changes of the CD spectrum were noticed following extensive ultrafiltration against the buffer.

6.2. Reactions with Representative Proteins

Subsequently, the reactions of either *Auoxo1* or *Auoxo6* with a few model proteins were carried out and analysed according to established experimental protocols of our laboratory [2,14,29]. In particular, these two compounds were challenged against human serum albumin (hSA), horse heart cytochrome c (cyt c), and bovine ubiquitin (Ubq, from red blood cells), and the respective reaction batches monitored spectrophotometrically over 24 h.

The spectral profiles of the reactions of *Auoxo1* with hSA, cyt c, and Ubq are suggestive of the occurrence of relatively slow reactions between *Auoxo1* and the various model proteins. Some common trends are easily identified in the resulting spectral profiles consisting of the progressive decrease of the typical bands of *Auoxo1* and of the appearance of new bands around 285 nm, characteristic of the free ligand. Thus, the obtained spectral patterns may be interpreted in terms of the progressive reduction of the gold(III) centres by protein side chains. A substantial analogy with gold(III) reduction produced by ascorbic acid is evident though the kinetics of the reduction process induced by proteins is significantly slower.

When *Auoxo6* was reacted with the same model proteins, somehow similar spectral patterns were found. Again, the progressive decay of the characteristic LMCT bands of the gold(III) chromophore was observed accompanied by the appearance of the bands at ca 280 nm assigned to the free

ligand. However, in the case of hSA and cyt c, these redox processes were found to be much faster than for *Auoxo1*. At the end of the process most of the added gold was found associated with the proteins. The spectral profiles for the reaction of *Auoxo1* and *Auoxo6* with BSA are reported in Fig. (**8**).

For both *Auoxo1* and *Auoxo6*, independent ICP-OES determinations were carried out on the final solutions, following 24 h of incubation at 37°C and extensive ultrafiltration against the buffer, working at a metallodrug/protein ratio of 1:1. ICP results pointed out that a very large percentage of total gold (>80%) remains in the upper fractions, tightly associated with either hSA or cyt c. At variance, in the case of ubiquitin, the percentage of gold that is eventually associated with the protein is only ca 50%.

Additional information on the nature of gold/protein adducts was derived from ESI MS measurements in the case of cyt c. ESI MS profiles were collected after reacting cyt c with either *Auoxo1* or *Auoxo6* (Fig. **9**), working at 1:1 *Auoxo*/cyt c ratios [2]. After 12 h incubation, cyt c was extensively ultrafiltered against the ammonium carbonate buffer and the ESI MS spectra of the upper fractions recorded.

In both cases, the final deconvoluted ESI MS spectra provided clear evidence of adduct formation. Remarkably, a few peaks were detected formally corresponding to the binding of a number of Au^{+} ions (ranging from 1 to 4) to the protein. A similar ESI MS behavior was previously reported by Sadler *et al*. for the $(Au(PEt_3)Cl)$/cyclophilin system [30]. It is remarkable that no sign of the bipiridyl ligand coordinated

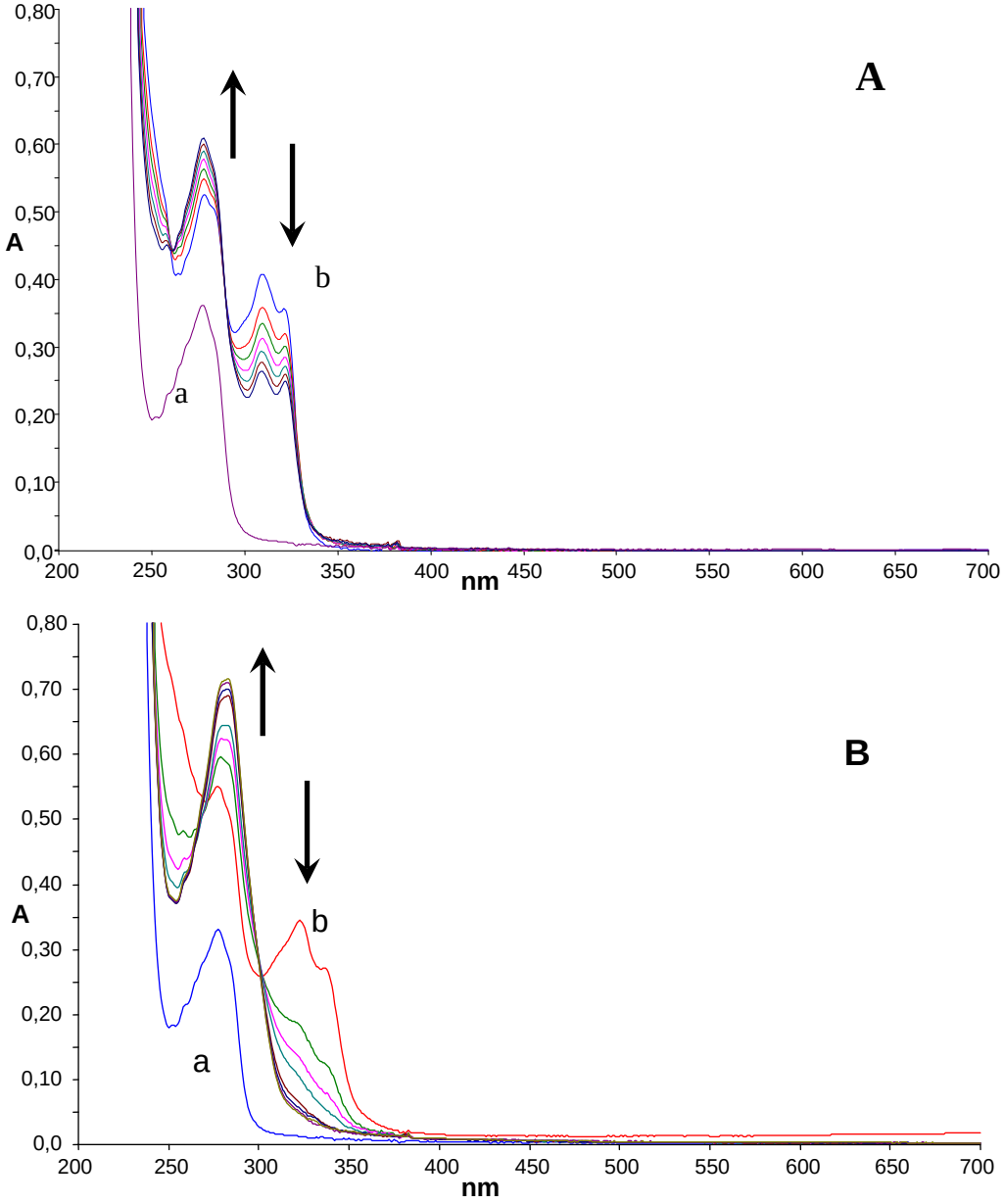

Fig. (8). Time-dependent spectral profiles for 1:1 *Auoxo*/human SA adducts. Spectra correspond to 10^{-5} M hSA before (a) and after (b) addition of *Auoxo1* (**A**) and *Auoxo6* (**B**). The further evolution over 24 h is reported at 37°C. The arrows indicate the changes occurring during this period.

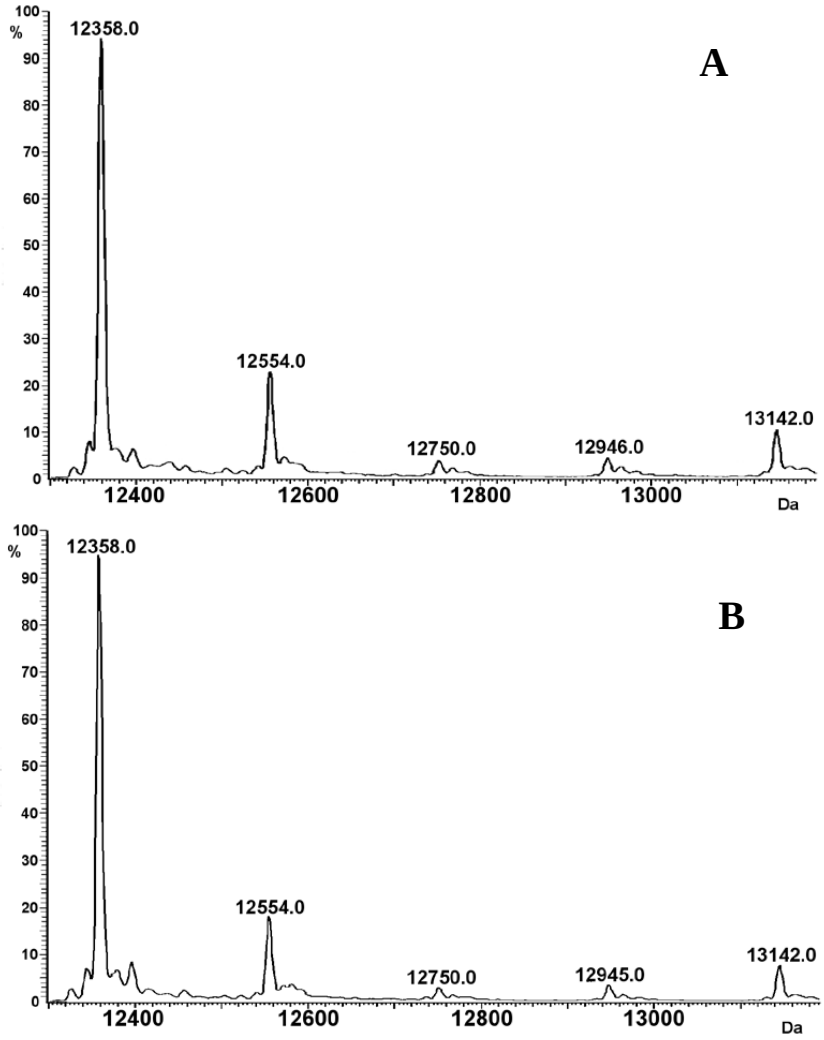

Fig. (9). Deconvoluted ESI MS spectra for cytochrome c adducts with Auoxo1 (**A**) and Auoxo6 (**B**).

to gold was found anymore, implying that the reduction process causes complete disruption of the starting dinuclear compound with cleavage of the oxo bridges, release of the bipyridyl ligand, and protein binding of the isolated gold ions.

7. CONCLUDING REMARKS

In recent years *Auoxos* have emerged as an innonative class of cytotoxic gold(III) compounds of potential interest for the development of new anticancer drugs. Notably, *Auoxos* are dinuclear gold(III) complexes characterised by an appreciable solubility and stability in physiological buffers. Cytotoxicity assays revealed that *Auoxos* display very attractive antiproliferative effects *in vitro*; however the pattern of the measured cytotoxicities is deeply different from that of CDDP suggesting the occurrence of a substantially different mechanism of action. Significant differences in the biological profiles of the various *Auoxos* were highlighted as well. A few targets emerged from COMPARE analysis of the antiproliferative data. In particular important proteins such as HDAC and PKC turned out to be likely targets and will be further investigated. Interaction studies of *Auoxos* with calf thymus DNA and with a few model proteins were carried out as well. Deeply different interaction modes with calf thymus DNA were highlighted for *Auoxo1* and *Auoxo6*. At variance, biophysical studies of their reactions with a few model proteins strongly suggested that these interactions are dominated by redox transformations. Evidence is provided that *Auoxos* are in most cases a source of gold(I) ions which may eventually bind a variety of protein targets. These findings are in accordance with the view that *Auoxos* behave as *prodrugs* and manifest a high reactivity with several proteins. On the ground of the above arguments *Auoxos* may be considered promising cytotoxic agents for further pharmacological testing and development. However, as these gold compounds typically manifest a high reactivity with biological molecules appropriate strategies might be implemented to control their reactivity through specific pharmaceutical formulations (e.g nanocapsules or liposomes). Also, “smart” strategies should considered for targeting these novel cytotoxic metallodrugs selectively to the tumor tissue.

REFERENCES

[1] Nobili S, Mini E, Landini I, Gabbiani C, Casini A, Messori L. Gold compounds as anticancer agents: chemistry, cellular pharmacology, and preclinical studies. Med Res Rev 2009; in the press.

[2] Casini A, Hartinger C, Gabbiani C, *et al*. Gold(III) compounds as anticancer agents: relevance of gold-protein interactions for their mechanism of action. J Inorg Biochem 2008; 102: 564-75.
[3] Messori L, Marcon G. Gold complexes as antitumor agents. Met Ions Biol Syst 2004; 42: 385-424.
[4] Ott I. On the medicinal chemistry of gold complexes as anticancer drugs. Coord Chem Rev 2009; 253: 1670-81.
[5] Tiekink ERT. Gold derivatives for the treatment of cancer. Crit Rev Oncol/Hematol 2002; 42: 225-48.
[6] Milacic V, Chen D, Ronconi L, Landis-Piwowar KR, Fregona D, Dou QP. A novel anticancer gold(III) dithiocarbamate compound inhibits the activity of a purified 20S proteasome and 26S proteasome in human breast cancer cell cultures and xenografts. Cancer Res 2006; 66: 10478-86.
[7] Saggioro D, Rigobello MP, Paloschi L, *et al*. Gold(III)-dithiocarbamato complexes induce cancer cell death triggered by thioredoxin redox system inhibition and activation of ERK pathway. Chem Biol 2007; 14: 1128-39.
[8] Wang Y, He QY, Sun RW, Che CM, Chiu JF. Isolation of cytoplasmatic proteins from cultured cells for two-dimensional gel electrophoresis. Cancer Res 2005; 65: 11553-64.
[9] Messori L, Abbate F, Marcon G, *et al*. Gold(III) complexes as potential antitumor agents: solution chemistry and cytotoxic properties of some selected gold(III) compounds. J Med Chem 2000; 43: 3541-8.
[10] Marcon G, Carotti S, Coronnello M, *et al*. Gold(III) complexes with bipyridyl ligands: solution chemistry, cytotoxicity, and DNA binding properties. J Med Chem. 2002; 45: 1672-7.
[11] Mendoza-Ferri MG, Hartinger CG, Mendoza MA, *et al*. Transferring the concept of multinuclearity to ruthenium complexes for improvement of anticancer activity. J Med Chem 2009; 52: 916-25.
[12] Farrell N. Polynuclear platinum drugs. Met Ions Biol Syst 2004; 42: 251-96.
[13] Bergamo A, Stocco G, Gava B, *et al*. Distinct effects of dinuclear ruthenium(III) complexes on cell proliferation and on cell cycle regulation in human and murine tumor cell lines. J Pharmacol Exp Ther 2003; 305: 725-32.
[14] Casini A, Cinellu MA, Minghetti G, *et al*. Structural and solution chemistry, antiproliferative effects, and DNA and protein binding properties of a series of dinuclear gold(III) compounds with bipyridyl ligands. J Med Chem 2006; 49: 5524-31.
[15] Gabbiani C, Casini A, Messori L, *et al*. Structural characterization, solution studies, and DFT calculations on a series of binuclear gold(III) oxo complexes: relationships to biological properties. Inorg Chem 2008; 47: 2368-79.
[16] Cinellu MA, Minghetti G, Pinna MV, *et al*. μ-Oxo and alkoxo complexes of gold(III) with 6-alkyl-2,2-bipyridines. Synthesis, characterization and X-ray structures. J Chem Soc Dalton Trans 1998; 11: 1735-42.
[17] A search in the Cambridge Structural Database (CSD v. 5.28; Allen, F. H. /Acta Cryst B/, *2002*, /B58/, 380) retrieved 11 hits of which only 3 have an OR bridge: one of these is /trans-/*4* (R = none), the other are hydroxo bridged complexes featuring Au…Au distances in the range 3.15-3.43 Å.
[18] Veiros LF, Calhorda L. How bridging ligands and neighbouring groups tune the gold-gold bond strength. J Organomet Chem 1996; 510: 171-81.
[19] Shaw III. CF. Gold-based therapeutic agents. Chem Rev 1999; 99: 2589-600.
[20] Skehan P, Storeng R, Scudiero D, *et al*. New colorimetric cytotoxicity assay for anticancer-drug screening. J Natl Cancer Inst 1990; 82: 1107-12.
[21] Casini A, Kelter G, Gabbiani C, *et al*. Chemistry, antiproliferative properties, tumor selectivity, and molecular mechanisms of novel gold(III) compounds for cancer treatment: a systematic study. J Biol Inorg Chem. 2009; 14: 1139-49.
[22] Paull KD, Shoemaker RH, Hodes L, *et al*. Display and analysis of patterns of differential activity of drugs against human tumor cell lines: development of mean graph and COMPARE algorithm. J Natl Cancer Inst 1989; 81: 1088-92.
[23] Huang RL, Wallqvist A, Covell DG. Anticancer metal compounds in NCI's tumor-screening database: putative mode of action. Biochem Pharmacol 2005; 69: 1009-39.
[24] Boyd MR, Paull KD, Rubinstein LR. In: Valeriote FA, Corbett T, Backer L (Eds) Cytotoxic anticancer models and concepts for drug discovery and development. Kluwer; Amsterdam, 1992; pp. 11-34.
[25] Fang XL, Shao L, Zhang H, Wang SM. Web-based tools for mining the NCI databases for anticancer drug discovery. J Chem Inf Comput Sci 2004; 44: 249-57.
[26] Witt O, Deubzer HE, Milde T, Oehme I. HDAC family: What are the cancer relevant targets? Cancer Lett 2009; 277: 8-21.
[27] Stallings-Mann M, Jamieson L, Regala RP, Weems C, Murray NR, Fields AP. A novel small-molecule inhibitor of protein kinase Ciota blocks transformed growth of non-small-cell lung cancer cells. Cancer Res 2006; 66: 1767-74.
[28] Messori L, Orioli P, Tempi C, Marcon G. Interactions of selected gold(III) complexes with calf thymus DNA. Biochem Biophys Res Commun 2001; 281: 352-360.
[29] Casini A, Gabbiani C, Mastrobuoni G, Messori L, Moneti G, Pieraccini G. Exploring metallodrug-protein interactions by ESI mass spectrometry: the reaction of anticancer platinum drugs with horse heart cytochrome c. ChemMedChem 2006; 1: 413-7.
[30] Zou J, Taylor P, Dornan J, Robinson SP, Walkinshaw MD, Sadler PJ. First crystal structure of a medicinally relevant gold protein complex: Unexpected Binding of $[Au(PEt_3)]^+$ to Histidine. Angew Chem Int Ed Engl 2000; 39: 2931-4.

Received: December 08, 2009 Revised: January 01, 2010 Accepted: January 15, 2010